Hindawi Publishing Corporation
Journal of Geological Research
Volume 2013, Article ID 805451, 12 pages
http://dx.doi.org/10.1155/2013/805451

Research Article

Multiphase Alkaline Basalts of Central Al-Haruj Al-Abyad of Libya: Petrological and Geochemical Aspects

Abdel-Aal M. Abdel-Karim,[1] El-Nuri M. Ramadan,[2] and Mohamed R. Embashi[2]

[1] *Geology Department, Faculty of Science, Zagazig University, Egypt*
[2] *Geology Department, Faculty of Science, El-Zawia University, Libya*

Correspondence should be addressed to Abdel-Aal M. Abdel-Karim; abdelaalabdelkarim@hotmail.com

Received 4 February 2013; Revised 10 April 2013; Accepted 12 April 2013

Academic Editor: Karoly Nemeth

Al-Haruj basalts that represent the largest volcanic province in Libya consist of four lava flow phases of varying thicknesses, extensions, and dating. Their eruption is generally controlled by the larger Afro-Arabian rift system. The flow phases range from olivine rich and/or olivine dolerites to olivine and/or normal basalts that consist mainly of variable olivine, clinopyroxene, plagioclase, and glass. Olivine, plagioclase, and clinopyroxene form abundant porphyritic crystals. In olivine-rich basalt and olivine basalt, these minerals occur as glomerophyric or seriate clusters of an individual mineral or group of minerals. Groundmass textures are variably intergranular, intersertal, vitrophyric, and flow. The pyroclastic, clastogenic flows and/or ejecta of the volcanic cones show porphyritic, vitrophric, pilotaxitic, and vesicular textures. They are classified into tholeiite, alkaline, and olivine basalts. Three main groups are recorded. Basalts of phase 1 are generated from tholeiitic to alkaline magma, while those of phases 3 and 4 are derived from alkaline magma. It is proposed that the tholeiitic basalts represent prerift stage magma generated by higher degree of partial melting (2.0–3.5%) of garnet-peridotite asthenospheric mantle source, at shallow depth, whereas the dominant alkaline basalts may represent the rift stage magma formed by low degree of partial melting (0.7–1.5%) and high fractionation of the same source, at greater depth in an intra-continental plate with OIB affinity. The melt generation could be also attributed to lithosphere extension associated with passive rise of variable enriched mantle.

1. Introduction

The volcanic rocks territory of Libya ranging in age from the Eocene to present day occur. The age of these predominantly basaltic rocks decreases from north to south. The Central Al-Haruj Al-Abyad (CHA) basalt flows cover the southern part of the Al-Haruj total volcanic province between 26°N and 26° 30′N latitudes and 16° 45′E and 18°E longitudes in the central Libya. It is featured by close structural and genetic relationship with the Al-Haruj al-Abyad total volcanic system, so the present authors adopt a similar classification of the volcanic pile as it had been elaborated in the previous works [1–3] distinguishing 4 major eruption phases and 11 subphases or flow units. The origin of the volcanism is still not clear.

The Al-Haruj flood basalt field (45,000 km^2) is the largest of four Tertiary to Recent volcanic provinces in central Libya [1] (Figure 1). The CHA falls within the Al-Haruj basalt field; it is located southwest of the main and youngest region of the field which is called Al-Haruj Al-Aswad. The main and youngest part, Al-Haruj Al-Aswad considered to be Holocene by Klitzsch [4], was recently dated between 4 and 0.5 Ma in its eastern part [5]. Al-Haruj Al-Abyad, located southwest of Al-Haruj Al-Aswad, was also studied [3, 6, 7] and dated Miocene to Pliocene (6–0.4 Ma, [8]). The entire Al-Haruj total volcanic area is significantly greater than the Tibesti volcanic region [4, 9]. At CHA, also the lava fields are the volumetrically most important features. The eruption of these masses is generally controlled by NW-SE major tectonic lines, which is probably related to the larger Afro-Arabian rift system. The structural control on the location of volcanic fields was variously interpreted. According to Goudarzi [10] and Woller and Fediuk [11], two major fault systems, NNW-SSE (Al-Haruj uplift) parallel to the Red Sea and NNE-SSW

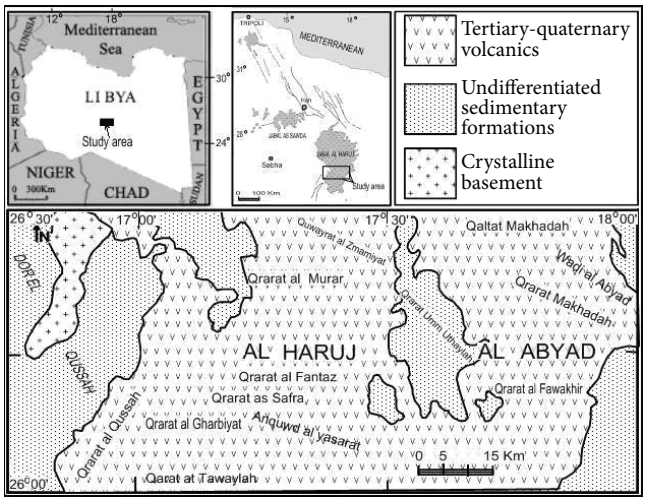

Figure 1: Location and generalized geological map showing the distribution of Al-Haruj Al-Abyad basalts, central Libya.

(Dür al Qussah fault zone) parallel to other African rifts, intersect in the Al-Haruj area, near the central part of Libya (Figure 1).

The Al-Haruj basalt province was examined by Klitzsch [4] as a minor and six major basalt lava flows. In CHA, Peregi et al. [2] followed the volcanological framework elaborated by Busrewil and Suwesi [1] distinguishing 6 volcanic phases subdivided together into 15 subphases or unit basalt flows.

The petrochemical studies on Al-Haruj province indicate that most volcanic rocks belong to the alkaline olivine basaltic suite and range in composition from basalts to hawaiite; however, a systematic compositional variation cannot be drawn [2, 5, 14–17]. In this respect, Al-Haruj volcanic province does not differ significantly from other large volume Tertiary volcanic suites in Libya [11, 14, 15, 18–21]. The region is a typical intraplate setting but counts among the volcano-capped swells randomly distributed on the African plate and inferred to be a result of hot spot activity [2, 16, 22, 23]. Many similarities can be found with other intraplate alkaline basaltic fields in northern Africa, such as the volcanic rocks of Meidob in NW Sudan [24] and the West Shalatein in the south Eastern Desert, Egypt.

The age of the volcanic area has been determined by combined paleomagnetic and K/Ar whole-rock age dating methods, giving ages between 6.0 and 0.3 Ma [1, 2, 5, 8].

In this paper, petrological and geochemical studies focus on CHA basalt flows in order to confirm their tectono-magmatic evolution and origin of volcanism.

2. Geology Background

Gabal Al-Haruj (1,200 m) in the central Libya occupies about 45,000 km^2, representing one of the largest volcanic provinces in West Africa. It is represented by the northern Al-Haruj Al-Aswad and the southern Al-Haruj Al-Abyad Mountains. The eruption of these masses is generally controlled by NW-SE major tectonic lines, which is probably related to the larger Afro-Arabian rift system.

The geology of CHA volcanic province is still under debate although it is widely discussed by several specialists [1, 2, 4, 15, 21, 25]. The following is a synopsis on the geology background of CHA volcanic province.

The volcanic lava flows of CHA province (Figure 1) are underlain by sedimentary sequence. The province is characterized by several volcanic structures like craters, maars, linear feeders, and so forth which are developed along nearly straight magma-tectonic lines. Small shield volcanoes and volcanic cones (about 60) are arranged following a WNW-ESE trend, 80 km long fissure system up to 700 m elevation and 8 km wide [2]. The volcanic sequence has an average thickness of a few tens of meters with the underlying Tertiary sedimentary strata cropping out frequently inside the extensive lava fields.

Four basalt lava flow phases are recorded in the concerned area. The division of the volcanic phases is based on similar principles that were developed by the earlier workers [1, 2, 4, 15, 21]. This division is basically based on the field observations together with trace elements chemistry.

2.1. Phase 1 Lava Flows (Early to Late Pliocene, 5.33–2.59 Ma). The first lava phase exposes all over the Haruj area except the more recent major volcanic centers. It extends along 55 km long and about 10–30 km wide NW-SE trending zone from Quwayrat al Zmamiyat to Qarat al Fawakhir plateau (Figure 1). Lavas of this phase appear also around the shield volcanoes Umm al Asal and near CHA. Sometimes, the low lands of these lavas are covered by more recent lava flows. This phase was subdivided into 3 subphases but their exact stratigraphic succession is still controversial [2]. These subphases basalts are coeval or merge one into another as well as the age dating and field observations do not allow any better constrain on their relationships. The subphasesoccur as massive, grey coloured, angular-blocky lava type (up to 2 meters diameter). They exhibit medium and vesicular textures and dominate around Wadi al-Abyad. Shield volcanoes are built up of similar lava flows, recoded at 10 km to the west of Qarat at Tawaylah. The Volcanic cones consist of variable sized scoria, welded scoria, and clastogenic lava flows. The pyroclastic beds (20–50 cm thick) consist mainly of spongy lavas and rare massive flows. Phase 1 lava flows are usually explosive due to their interaction with the water-saturated Tertiary sediments of the late Miocene lacustrine basin.

2.2. Phase 2 Lava Flows (Late Pliocene, 3.60–2.58 Ma). The phase 2 lavas cover all over CHA plateau. They are probably derived from the already mentioned 80 km long fissure volcanic system and its associated volcanoes. Numerous small parasite craters and vents are associated with the main volcanic centers which may have also produced significant lava. The present phase has been divided into 2 subphases which are different in their ages and field positions. The subphases occur as homogenous flood basalts of grey coloured vesicular lava of large blocks and slabs (20–50 cm). They exhibit fine, vesicular, and porphyritic textures. Shield

volcanoes are larger than those of phase 1, generally having 5–8 km diameter and quite flat surface, and built up of highly vesicular, spongy lava flows, and blocky lava (north Qarat at Tawaylah and near Qarat al-Fawakhir). The Volcanic cones form more than 20 cones which dispersed along a 10 km wide and 80 km long zone of the main fissure, built up of scoria, spatter and clastogenic lava flows.

2.3. Phase 3 Lava Flows (Early Pleistocene, 1.81–0.78 Ma). The phase 3 is divided into 3 subphases of variable distribution. The subphases expose as black basaltic lavas, usually covered by flows of subphase 4.1. It forms vesicular and blocky surface baltat (50 m–1 km), roughest types of large, subangular blocks or moderate relief, smooth, flat surface plateau of vesicular blocks of spongy lava. Sometimes, they are overlain by basalt lavas of phase 4 and overlain the flood basalts of subphases 1.2 and 1.3.

Their surfaces are hidden by thin, discontinuous sand cover which frequently covers the flows of phase 2. Shield volcanoes are numerous (about 20) and form continuous ridge associated with fissure zone. In the later zone, the shield volcanoes form a WNW-ESE chain (80 km long, 8 km wide), which are associated with scoria, spatter, and clastogenic cones, such as Qarat al-Gharbiyat (660 m), Qarat Safra (625 m), and al-Qaraniyat (700 m). Pyroclastic breccias, welded agglutinate, spatter deposits, reddish brown scoria, and lapillis are usually common. The volcanic cones are less than 1 km in diameter with 30–50 m craters. Two types of volcanic cones were recognized (e.g., Strombolian and Hawaiian), made up of pyroclastic materials and clastogenic lava flows.

2.4. Phase 4 Lava Flows (Early to Middle Pleistocene, 1.80–0.13 Ma). This phase is classified into 3 subphases. In CHA fissure volcanic zone, the subphase 4 is usually less distributed and occurs as small lavas associated with volcanic centers producing minor lavas of a few square kilometers. The subphases form a wadi filling thin basalt flows of ten meters wide and are composed of vesicular lavas forming rough hills of tumuli, ridge, and steep lava scarps. They form 3–6 km wide and 7–15 km long lava fields. They usually form small "baltat" of 100–200 m magnitude. The Volcanic cones range from 0.5–3 km in dimensions; their craters are 50–70 m in diameter mostly filled back with debris (south Qarat al-Fantazi and Anquwd al-Yasarat). They consist of welded scoria, agglutinate, spatter, and clastogenic lavas with 20–50 cm thick bedding.

K-Ar age dating yielded ages for the different volcanic phases ranging from 5.04 ± 0.23 Ma to 0.3 ± 0.2 Ma, for example, they have belonged to Pliocene to Pleistocene [2, 5].

The present volcanic flows are overlain unconformably by Pleistocene sandy limestone and younger Quaternary sediments mainly of clastic rock formation lacustrine, playa, wadi deposits, sebha, deluvial, proluvial, and eolian clastics. The oldest basalts overlie Miocene clastic carbonate sediments, while the youngest basalts are confined to paleo-wadis where they cut Quaternary sediments [5].

Many basaltic and phonolitic dykes and smaller lava plugs cut across the present basaltic rocks and/or the Tertiary sedimentary rocks and occur detached from the main zone. Cvetković et al. [5] reported that these dykes usually have a NW-SE strike and dip toward the NE and SW (first system) and NNE, SSW, or S (second system). The first system coincides with the strike of the major fault structures and tension fractures in both structural levels. The second system has an acute angle to the first system, and it might represent pinnate systems related to the post-Lower Miocene sinistral strike slip activity of NW-SE striking faults.

3. Petrographic Features

The basalts of CHA are dense, dark grey to black in color, and range in grain size from medium to fine. Their mineralogical composition varies from olivine-rich and/or olivine to normal basalts and/or dolerites. Some of these basalts have undergone secondary alteration. Based on the chemical analysis, they are classified into dominant alkali olivine basalts and basanites with minor olivine tholeiites.

The basaltic rocks of flow phases consist mainly of variable olivine, clinopyroxene, plagioclase, and glass. Accessory minerals include titanomagnetite. Iddingsite, calcite, serpentine, and zeolite are the main secondary minerals. Olivine, plagioclase, and clinopyroxene form abundant porphyritic crystals. In olivine-rich basalt and olivine basalt, these minerals occur as glomerophyric or seriate clusters of an individual mineral or group of minerals. The groundmass consists of a plexus of plagioclase laths, clinopyroxene and olivine granules, small stumpy prisms and granules of Fe-Ti oxides, and interstitial glass, calcite, and zeolite. Groundmass textures are variably intergranular, intersertal, vitrophyric, and hyalopilitic. Dictytaxitic and flow textures are also observed.

Olivine occurs as early formed rounded grains or as idiomorphic phenocrysts. In the average basalts, it forms 8% of the rocks, but it reaches 13% in the olivine basalt and a maximum of 26% in the olivine-rich dolerite and basalt. Olivine is mostly fresh, but in some cases it is altered to iddingsite and/or serpentine.

Clinopyroxene occurs as phenocrysts and as granules in the groundmass. It increases in amount from 19% in the olivine-rich dolerite and basalt to 27% in the olivine basalt and 45% in the average basalt. It is usually zoned, with augite cores followed by titanaugite rims forming typical hourglass and sector zoning.

The clinopyroxenes of phases 1 and 2 exhibit a tholeiitic character, while those of the more voluminous phases 3 and 4 show an alkaline affinity [7].

Plagioclase occurs either as phenocrysts or as a major constituent of the groundmass. It varies from 17% in the olivine-rich dolerite and basalt to 38% in the olivine basalts and 51% in normal basalts. Plagioclase is mostly zoned and/or twinned and ranges in composition from labradorite (olivine-rich dolerite) through labradorite-andesine (olivine basalt) to labradorite-oligoclase (normal basalt).

Opaques are relatively abundant (8%) and form granules and microcrysts with occasional skeletals penetrating the

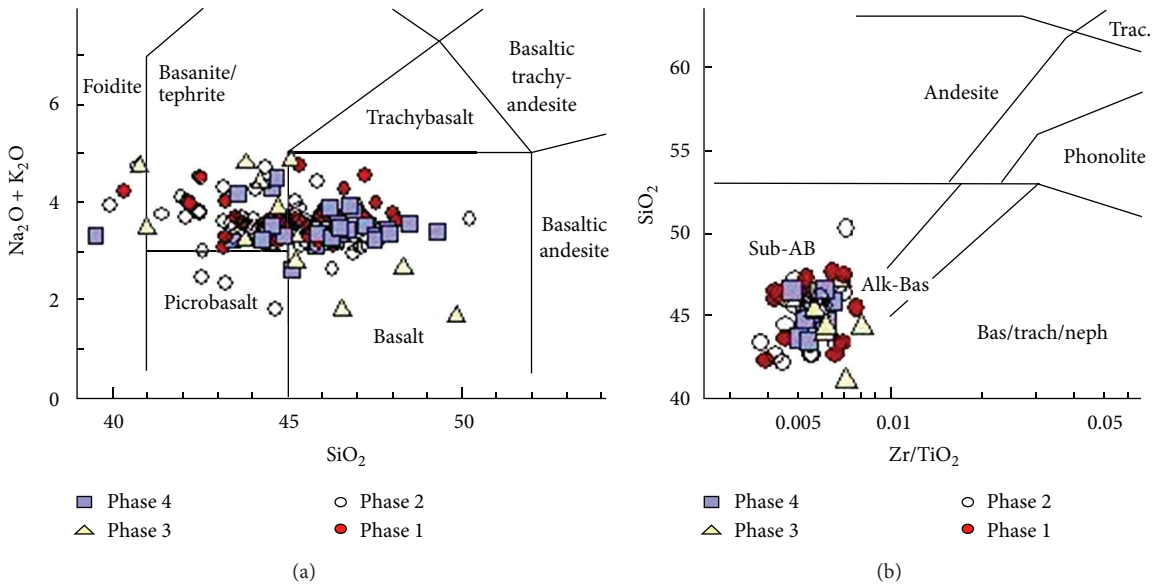

FIGURE 2: Classification of CHA basalts on SiO_2 versus $Na_2O + K_2O$ diagram of Le Bas et al. [12] and Zr/TiO_2 versus SiO_2 diagram of Winchester and Floyd [13].

silicate minerals. They appear to be normal magnetite and ferri-ilmenite or a mixture of both (titanomagnetite).

The volcanic cones of phase 1 and phase 2 occur as volcanic lithic fragments of olivine basalts that belong to the pyroclastic materials and clastogenic flows or as ejecta which show porphyritic vitrophric to pilotaxitic texture and vesicular structure. They consist mainly of olivine phenocrysts (15–22% in phase 1 to 10–13% in phase 2), clinopyroxene (5–30% in phase 1 to 30–35% in phase 2), plagioclase (5–20% in phase 1 to 15–20% in phase 2), and Fe-Ti oxide (4–8% in phase 1 to 5–9% in phase 2) together with variable glass. The olivine occurs as subhedral to euhedral phenocrysts (up to 1.5 mm long) or as anhedral to subhedral fine grained groundmass (up to 0.5 mm). The clinopyroxene forms subhedral crystals of augite or anhedral microlites in the groundmass. The plagioclase forms long, needle-shaped microcrysts (0.05 mm long) embedded in a glassy slightly devitrified groundmass.

The volcanic cones of phases 3 and 4 are mostly the pyroclastic materials which exhibit porphyritic hyalopilitic to vitrophric texture. They are composed mainly of olivine phenocrysts (15–18% in phase 3 to 25–33% in phase 4), clinopyroxene (2–6% in phase 3 to 12–16% in phase 4), plagioclase (5–13% in phase 3 to 40–44% in phase 4), and Fe-Ti oxide (6–10% in phase 3 to 3–6% in phase 4) together with glass and calcite thatoccur as variable amounts.

4. Geochemistry

Two hundred and twenty four samples from the studied basaltic flows of CHA were analyzed for their major element contents (including Sr and Ba). Also, fifty of these samples were analyzed for the trace elements. The major element data were provided by Industrial Research Center (Tripoli), while the trace elements by Hungarian Geology Institute

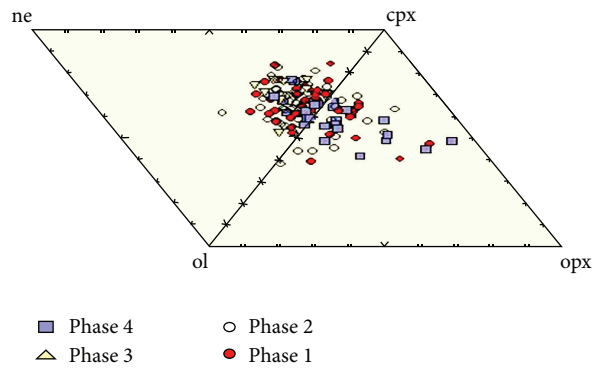

FIGURE 3: Normative nepheline (ne), olivine (ol), diopside (cpx), and hypersthene (opx) basalt tetrahedron diagram for the studied CHA basalts.

(Budapest). The analyses were carried out by ICP and ICP-MS methods, respectively. Statistical parameters of the major and trace elements analyses of the present basalt phases are reported in Table 1.

4.1. Classification. The adopted nomenclature based on chemical classification of the alkali-silica (TAS) diagram of Le Bas et al. [12] and Winchester and Floyd [13] are used to categorize the volcanic flows of CHA. Figure 2 reveals that most analyzed samples lie in the fields of basalt and basanite, except a few samples fall in foidite and picrobasalt field (Figure 2(a)). Moreover, the data points exist in the alkali basalt and subalkali (tholeiitic) basalt fields (Figure 2(b)). The basalts of phase 3 are mostly nepheline-normative alkaline basalts (ne = 0–7), whereas most samples of phases 1, 2, and 4 are scattered along nepheline-normative alkaline basalts (ne = 0–15) and hypersthene-normative ol-tholeiites

Table 1: Statistical parameters of the major and trace elements analyses of four phases of the central Al-Haruj al-Abyad basalt flows, central Libya.

	Phase 1			Phase 2			Phase 3			Phase 4		
	No.	Range	Mean	No.	Range	Mean	No.	Range	Mean	No.	Range	Mean
SiO_2	63	40.3–48.1	45.5	89	39.95–50.21	45.07	40	40.8–49.8	45.4	32	39.5–49.3	45.85
TiO_2	63	1.66–3.00	2.09	89	1.36–3.34	2.19	40	1.47–2.96	2.159	32	1.70–0.7	2.01
Al_2O_3	63	10.24–15.2	13.1	88	9.58–15.50	12.58	40	9.64–14.7	12.76	32	10.5–14	12.61
Fe_2O_3	63	10.50–14.4	12.7	89	11.08–14.21	12.76	40	10.6–14.5	12.94	32	11.8–13.9	12.65
MnO	63	0.06–0.40	0.17	19	0.07–0.35	0.17	40	0.10–0.38	0.174	32	0.13–0.35	0.167
MgO	63	5.63–12.7	9.46	19	8.17–13.97	10.92	40	5.9–13.5	9.79	32	6.74–12.6	9.61
CaO	76	8.55–13.8	10.4	19	8.37–12.20	10.88	40	8.66–12.9	10.44	32	8.68–11.7	10.18
Na_2O	47	2.11–3.63	2.85	19	1.64–3.60	2.62	18	1.21–3.89	2.74	26	2.13–3.30	2.77
K_2O	76	0.21–1.34	0.73	19	0.42–1.30	0.83	40	0.27–1.11	0.72	32	0.49–1.20	0.73
P_2O_5	76	0.10–0.82	0.32	19	0.16–0.54	0.32	40	0.17–0.81	0.37	32	0.16–0.60	0.34
LOI	75	0.12–3.89	1.35	19	0.04–2.97	1.61	38	0.12–3.56	1.34	32	0.20–2.80	1.34
SO_3	76	0.02–3.17	0.75	19	0.04–1.14	0.42	40	0.05–2.10	0.89	32	0.21–2.53	1.04
Sr	14	85–454	1448	19	85–4784	1083	10	293–2007	852	7	190–2316	702.8
Ba	14	170–1718	679.9	19	118–2782	1088	10	150–4166	1097	7	150–1616	664.5
As	14	0.70–1.6	1.05	19	0.10–3.80	1.36	10	1.00–2.13	1.31	7	1-1	1
Rb	14	8.40–21	13.8	19	12–19.80	15.85	10	5.18–25.6	16.1	7	11.8–21	16.47
Y	14	14–18	15.7	19	13.5–18.30	15.78	10	16.3–20	18	7	15.1–17.5	16.36
Zr	14	107–147	124	19	109–159.00	128.8	10	132–187	157.7	7	119–144	132
Nb	14	19–29	23.9	19	24.7–35.40	29.63	10	35.2–51	44.39	7	32–41.80	35.41
Cs	14	0.24–0.34	0.25	19	0.10–0.34	0.247	10	0.24–0.40	0.271	7	0.24–0.25	0.24
La	14	13.30–18	15.8	19	19.50–25.2	22	10	24.3–35.1	29.95	7	24–27.7	25.64
Ce	14	28.4–37	32.5	19	4.30–56.4	40	10	47.7–72.4	60.45	7	33–54.4	46
Pr	14	3.60–4.9	4.26	19	4.38–109	11	10	6.1–8.96	7.587	7	4.2–6.86	5.97
Nd	14	16.0–21.8	18.6	19	18.40–29.3	23.2	10	25.7–35.5	30.96	7	17.7–30.3	24.88
Sm	14	3.98–5.3	4.62	19	1.00–6.63	5.07	10	5.98–8.06	6.992	7	4.4–6.4	5.46
Eu	14	1.25–1.9	1.53	19	1.44–12	2.34	10	1.8–2.75	2.224	7	1.54–2.06	1.83
Gd	14	3.72–5	4.41	19	3.80–15.2	5.43	10	5–7.40	6.039	7	4.15–6.5	4.98
Tb	14	0.57–0.85	0.71	19	0.49–109	6.80	10	0.79–1.1	0.933	7	0.67–1.1	0.80
Dy	14	3.10–4.00	3.55	19	2.98–19.6	4.58	10	3.65–5.30	4.434	7	3.18–4.24	3.74
Ho	14	0.61–0.90	0.71	19	0.60–1.00	0.75	10	0.60–1.05	0.814	7	0.55–0.85	0.71
Er	14	1.37–1.78	1.58	19	1.32–12	2.15	10	1.36–2.14	1.685	7	1.59–1.8	1.67
Tm	14	0.18–0.34	0.24	19	0.17–15	1.03	10	0.16–0.33	0.236	7	0.2–0.34	0.26
Yb	14	1.10–1.49	1.32	19	1.10–109	7.01	10	1.18–1.80	1.365	7	1.01–1.5	1.28
Lu	14	0.16–0.3	0.21	19	0.15–19.6	1.23	10	0.14–0.26	0.204	7	0.17–0.28	0.21
Hf	14	2.20–3.4	2.75	19	1.0–3.8	3.02	10	2.80–4.30	3.48	7	2.4–3.3	2.95
Ta	14	1.40–2.52	2.02	19	1.87–12	3.18	10	3.12–4.10	3.69	7	2.1–4.3	3.04
Th	14	1.18–2.7	1.91	19	1.85–4.7	2.72	10	2.42–4.70	3.55	7	2.1–3.9	2.94

No.: number of analyses, LOI: loss on ignition.

(hy = 0–32) (Figure 3). However, a clear distinction between four phases of basaltic flows is not very clear (Table 1), especially in some major elements probably due to the role of mobility and leaching during alteration.

4.2. Major Elements Variation. The concentrations of major elements show no observable correlations with SiO_2. They demonstrate either large scattering, for instance, Na_2O, K_2O, and TiO_2, or uniform contents (e.g., CaO, MgO, or P_2O_5) probably due to their mobility and/or leaching during alteration. However,some elements are much better illustrated (see Figure 4). The Al_2O_3 is positive, while TiO_2, CaO, and MgO are negative correlated with SiO_2.

These variation trends in the major elements cannot be explained by simple fractional crystallization process but could be attributable to different degrees of partial melting

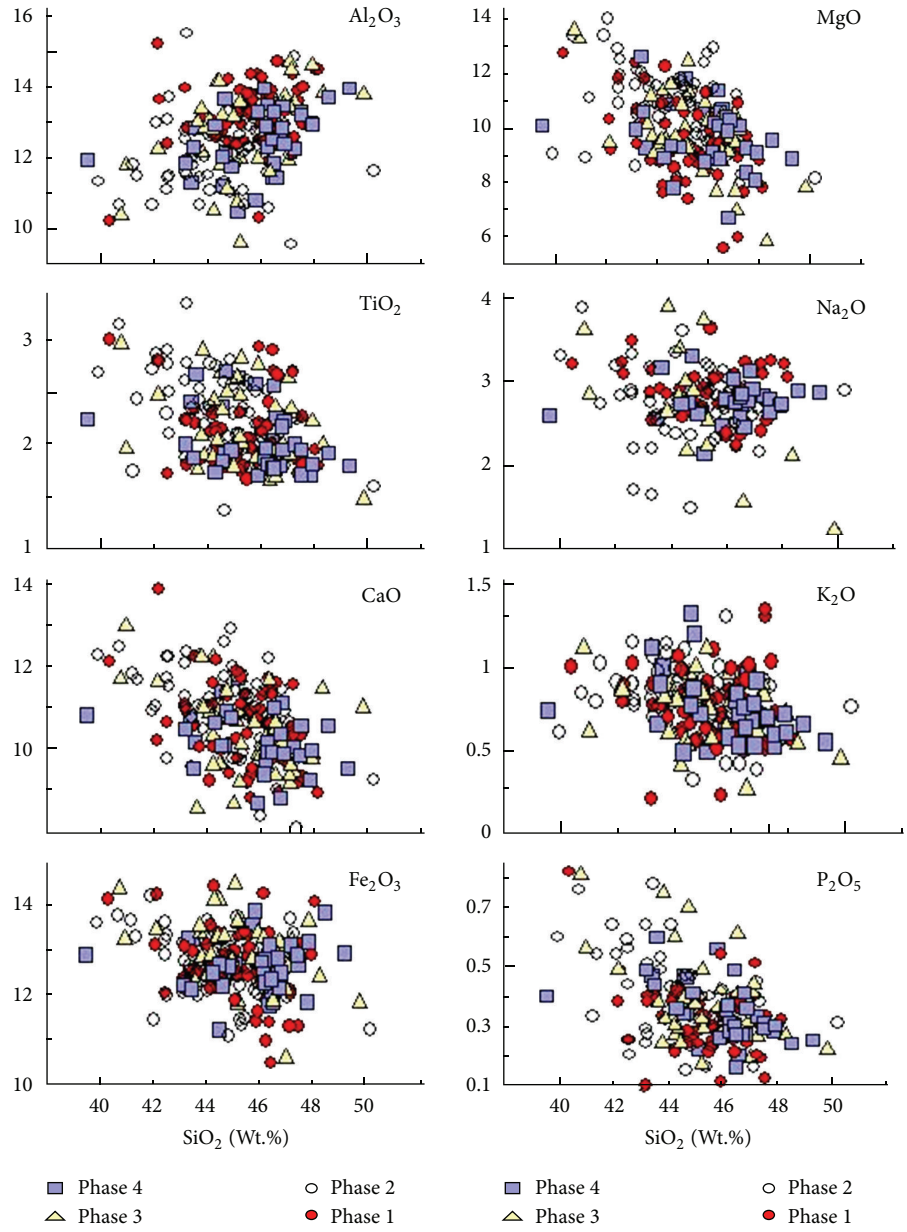

FIGURE 4: Variation diagrams of SiO_2 versus oxides for the studied CHA basalts.

and a possibly to different mantle sources [2]. The rough negative correlation between alkalis and SiO_2 in the basalts indicates that the different phases can be related by different degrees of partial melting rather than fraction crystallization.

4.3. Trace Elements Variation. The concentrations of all trace elements are relatively uniform. This is in accordance with essentially similar mineral compositions, textural characteristics, and some major element compositions displayed by these basalts irrespectively which volcanic phase and/or unit they belong. This implies that the studied basalts are petrogenetically related and may have originated by melting of a similar source and that they underwent similar differentiation processes. The interelemental relations between lanthanum and some trace elements are shown in Figure 5. La contents may reflect the degree of partial melting: mafic rocks of small La values could be generated by small degree of partial melting, while mafic rocks of high La values could originate by higher degree of partial melting as well as progressive fractionation. Rb, Y, Nb, Zr, Hf, Ta, Th, Ce, Nd, and Sm exhibit clear positive correlation with the La, which is consistent with the influence partial melting process.

The studied basalt flows can be classified into 3 main mafic groups based on their trace elements composition:

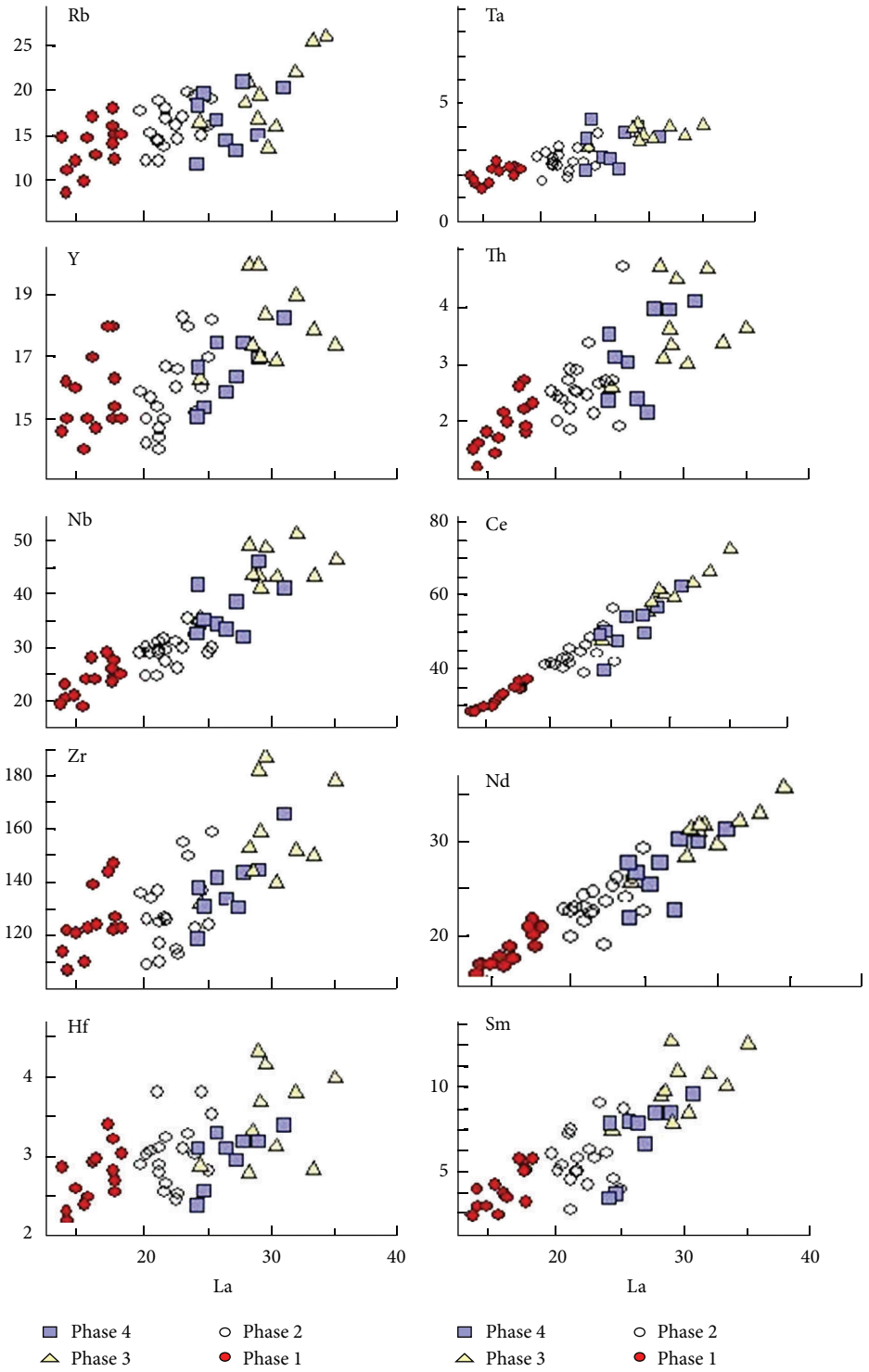

Figure 5: Variation diagrams of La versus trace elements for the studied CHA basalts.

(1) basalt of phase 1, (2) basalts of phase 2, and (3) basalts of phases 3 and 4. Figure 5 shows progressive increases in these elements from the basalts of phase 1 through phase 2 to basalts of phases 3 and 4, suggesting that the basalts of phase 1 haveundergone only slight olivine ± clinopyroxene fractionation and are close to the primary magma. Basalts of phases 3 and 4 have undergone moderate fractional crystallization.

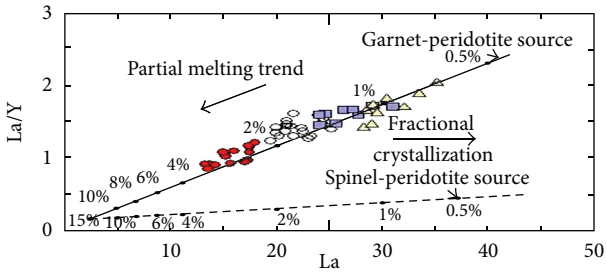

Figure 6: La versus La/Y diagram for the studied CHA basalts. Primitive mantle composition and distribution coefficients of Mckenzie and O'nions [26] are used, together with non-modal batch partial melting model, garnet peridotite and spinel peridotite source rocks, respectively. Numbers denote the degree of partial melting.

Moreover, it is useful to study the genesis of mafic magma using some incompatible trace elements as suggested by Minster and Allègre [30], Treuil et al. [31], and Harangi [16]. This can appear in the very good positive correlation between Y versus La (Figure 6). This linear relationship, moreover, could indicate both degrees of partial melting and different degrees of fractional crystallization [2, 16].

Therefore, it can be concluded that the variation of the trace elements and some major elements reveal that the chemical composition of the studied basalts was controlled essentially by different degrees of partial melting of similar mantle source region. The phases 3 and 4 basalts were generated by smaller degrees of partial melting, whereas the phase 1 basalts have been formed by the largest degrees of partial melting. The phase 2 basalts show mixed character between the former two groups.

5. Discussion and Conclusion

The available geochemical data allow discussion of some important petrogenetic aspects of the origin and evolution of the CHA. In the following sections we first discuss possible processes that could have been responsible for modification of primary melts, and then we elaborate some aspects of partial melting processes and characteristics of the mantle source. By combining this evidence and the evidence from geological data we provide some conclusions regarding petrogenetic implication.

5.1. Partial Melting versus Fractional Crystallization. Two main petrogenetic processes, for example, the partial melting and the fractional crystallization, can be distinguished using La versus La/Y [2, 16, 25, 31]. The degree of partial melting strongly influences the La/Y ratio, whereas the fractional crystallization commonly does not change the La/Y ratio. Figure 6 reveals that the variation trend of the studied basalt flows can be best explained by the different degrees of partial melting. Based on the direct quantitative petrogenetic modeling, we suggest a moderately enriched mantle source in the garnet stability field (deep than 50 km) and 0.7 to 1.5% melting for the phases 3 and 4 and 1.5–3.5% partial melting for the primary magmas of phases 1 and 2. Although phase 1 basalts have higher values of partial melting (2.0–3.5%) than other phases, these values are lower than those recorded for tholeiitic affinities. However, these values are slightly lower than those recorded for the eastern part of the Al-Haruj volcanic flows (5%) [5].

Petrographic evidence, such as olivine-phyric textures and the presence of glomerophyric aggregates, suggests that fractional crystallization has played an important role in magmatic differentiation of these basalts. Positive correlations between Ni contents and concentrations of MgO, TiO_2, and Cr (Table 1) suggest that olivine alone played a role of fractionation. The role of plagioclase fractionation is negligible or can be completely ruled out because of the absence of Eu anomaly (see also Figure 8) and because of the lack of correlation between Al_2O_3 and MgO contents.

The variations of incompatible trace element contents are given with respect to the concentrations of lanthanum because this trace element is found to be most incompatible in the studied rock suite. Namely, in an element-element diagram of two elements of identical incompatibility the slope and intercept of the linear regression should be unity and zero, respectively. On the other hand, a difference in incompatibility should result in a change of the slope and in an increase of the intercept on the axis of the less incompatible element. In such a way, the relative degree of incompatibility of other elements can be estimated by comparing their intercepts in element-element diagrams [32]. Figure 5 shows that there is a good correlation of the contents of all the presented trace elements with La concentrations. A positive correlation between the lanthanum concentrations and concentrations of other incompatible elements suggests that (i) all these rocks were likely derived from magmas which came from a similar source, and (ii) the observed variations were most likely produced by difference in degree of partial melting [5]. The variation patterns on La versus trace element ratio (e.g., La/Y, Figure 6) plots also support the hypothesis that partial melting was playing essential role in governing the absolute and relative abundance of incompatible elements. In addition, the observed negative correlations of Fe_2O_3 contents with silica contents (Figure 4) can be explained by varying degrees of melting caused by variable melting depths [33, 34]. This is consistent with the data given by Bardintzeff et al. [17] on alkaline volcanism between Al-Haruj and Waw an Namus (southern Libya) who attributed them to variable degrees of partial melting of mantle source with depth of melting between 80 and 150 km.

5.2. Tectono-Magmatic Setting. Using the discriminate Zr-Nb-Y diagram after Meschede [27] (Figure 7), the examined CHA basalts plot in the field of intraplate alkaline basalts. Moreover, the plots of the present data on the La-Y-Nb diagram of Cabanis and Lecolle [28] reveal that they are similar to the alkaline continental rift basalts (Figure 7).

5.3. Magma Sources and Petrogenetic Implication. On the chondrite normalized REE patterns (Figure 8), after Sun and McDonough [35], the basalts of phase 1 show a slight

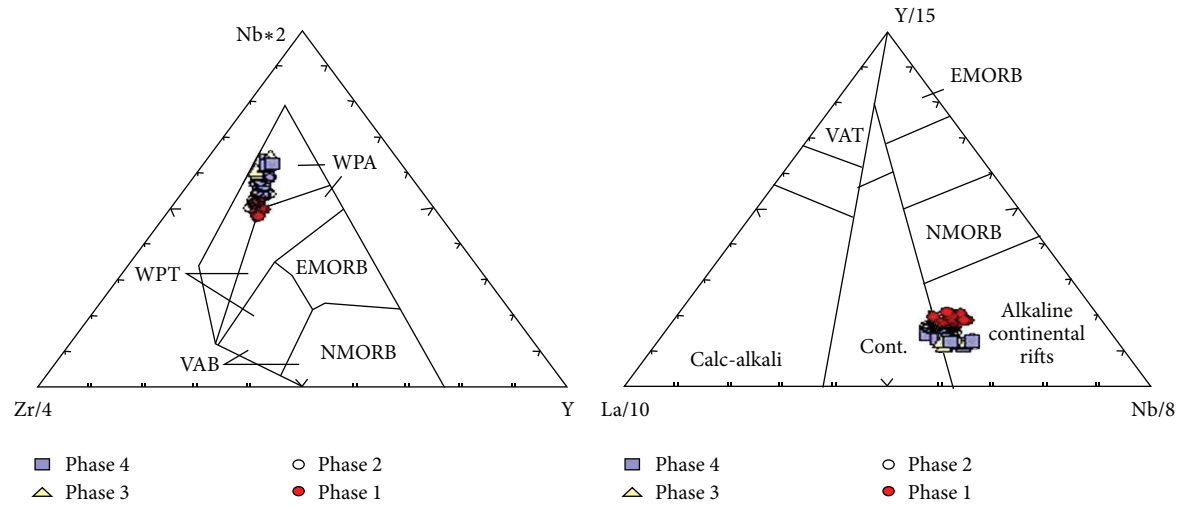

Figure 7: Plots of the CHA basalts on Nb-Zr-Y diagram after Meschede [27] and La-Y-Nb diagram after Cabanis and Lecolle [28].

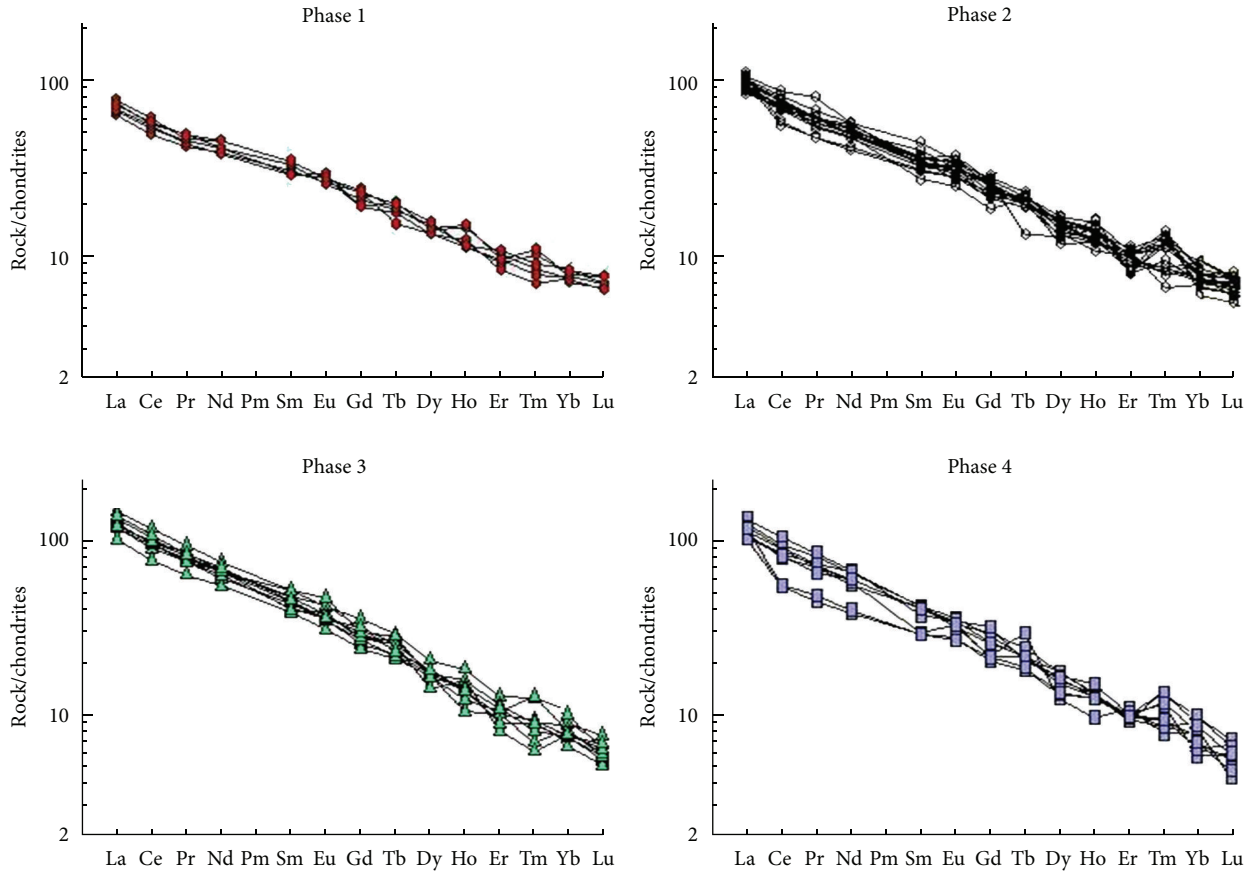

Figure 8: Chondrite normalized REE patterns for the studied CHA basalts.

enrichment of the LREEs and a slight depletion of the HREEs, with fair (or absence of –ve) Eu anomaly. This feature emphasizes their primitive source (garnet lherzolite origin) and the absence of plagioclase in the early crystallization process. On the other hand, the basalts of phases 3 and 4 show a more enrichment of the LREEs and a more depletion of the HREEs, without a clear –ve Eu anomaly. This feature may reveal their slight fractional crystallization process. The REEs

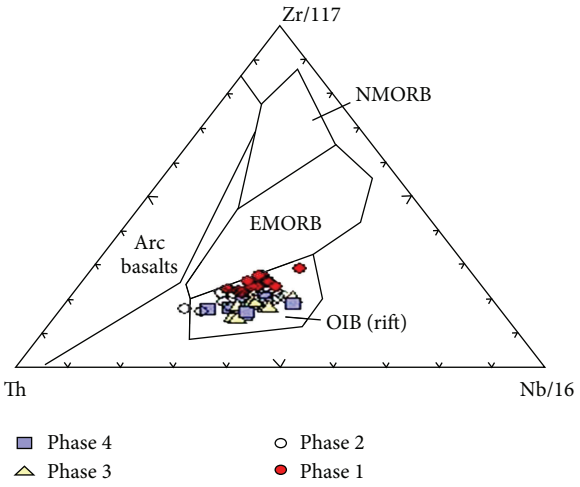

Figure 9: Plot of the CHA basalts on Th-Zr-Nb diagram after Wood et al. [29].

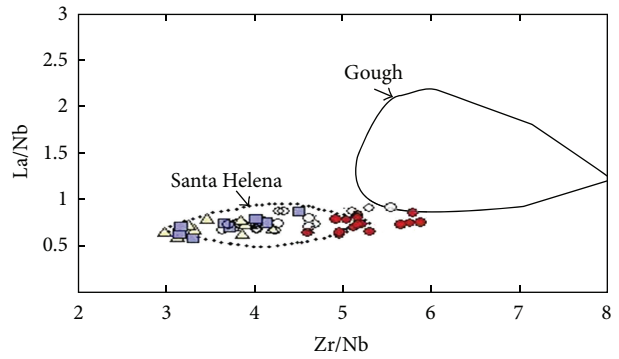

Figure 10: Zr/Nb versus La/Nb diagram of the CHA basalts. The fields of Santa Helena and Gough are based on the samples recorded in the GEOROC database (http://georoc.mpch-mainz.gwdg.de/georoc/).

pattern of phase 2 have intermediate affinity between the two former groups.

Moreover, a gradual progressive enrichment in LREEs and a regressive depletion in HREEs from basalts of phase 1 through phase 2 to phases 3 and 4. This feature probably indicates, again, their variable degrees of partial melting of the asthenosphere.

The extrusive environment of CHA basalts indicates that their eruption is related to the ocean island basalts (OIB) by rifting process [29] (Figure 9).

It is clear from the figures that the present basalts evolved by variable partial melting from variable patches of primary magma formed in within-plate setting in the upper mantle, without contamination by crustal material. These data are similar to that given by Bardintzeff et al. [17] for the volcanism between Al-Haruj and Waw an Namus (southern Libya). Such basaltic magmas are thought to be similar to the ocean island basalt (OIB), and they serve commonly as reference material for continental mafic rocks.

In spite of the general genetic similarity of the OIB magmas, they exhibit fairly wide trace element and radiogenic isotope composition [36]. This feature can be attributed to their derivative from heterogeneous mantle source with low and various degrees of partial melting. The Santa Helena [37] and the Gough basalts [38] are the two end members of the OIB. The two types have high mg values ($Mg/Mg+Fe^{2+}$) = 0.65–0.69 revealing that they did not undergo significant crystal fractionation which reflects their primary magmas. The mg no. values (0.58–0.69) and the trace element ratios of the CHA basalts are analogous to the Santa Helena-type OIB (Figure 10), which is called also HIMU (high μ) OIB [39].

The HIMU OIB is usually thought to be connected to the active mantle upwelling (mantle plume). However, other authors invoke CO_2-bearing mantle metasomatism to produce this geochemical character (i.e., [35, 40]). The negative K-anomaly in the primary mantle normalized trace element diagrams is also in a harmony with the Santa Helena-type affinity. This feature indicates that a K-bearing phase (either amphiboles or phlogopite) remained in the mantle source after the melting event. In any case it implies that the mantle region contained hydrous mineral, which could enhance the partial melting decreasing the solidus temperature of the peridotite. Therefore, it is not necessary to invoke an active mantle plume to generate the basalt volcanism in this area, but the melt generation could be also attributed to lithospheric extension associated with passive upwelling of variously metasomatized upper mantle. The role of lithospheric mantle sources enriched by melts derived from sublithospheric convecting mantle at sometime in the past has been reported by many studies (see [5, 41] and references therein).

Acknowledgments

The first author deeply appreciates the Industrial Research Centre, Tripoli, Libya, for kindly providing the chemical analysis. Careful reviews by Professor J.M. Bardintzeff and Professor K. Nemeth, greatly helped to improve this paper.

References

[1] M. T. Busrewil and K. S. Suwesi, "Explanatory booklet for the Geological Map of Libya (1:250, 000). Sheet," Al Haruj Al Aswad NG, (33-4), Industrial Research Centre, Tripoli, Libya, 1993.

[2] Z. Peregi, G. Y. Less, G. Y. Konrad et al., "Explanation booklet, Geological map of Libya, 1:250, 000. Sheet," Al Haruj Al Abyad NG 33-8, Industrial Research Center, Tripoli, Libya, 2003.

[3] K. Németh, "The morphology and origin of wide craters at Al Haruj al Abyad, Libya: maars and phreatomagmatism in a large intracontinental flood lava field?" *Zeitschrift fur Geomorphologie*, vol. 48, no. 4, pp. 417–439, 2004.

[4] E. Klitzsch, "Der Basaltvulkanismus des Djebel Haroudj Ostfezzan/Libyen," *Geologische Rundschau*, vol. 57, no. 2, pp. 585–601, 1968.

[5] V. Cvetković, M. Toljić, N. A. Ammar, L. Rundić, and K. B. Trish, "Petrogenesis of the eastern part of the Al Haruj basalts (Libya)," *Journal of African Earth Sciences*, vol. 58, no. 1, pp. 37–50, 2010.

[6] K. H. Ne'meth, K. S. Suwesi, Z. Peregi, Z. Gula'csi, and J. Ujsza'szi, "Plio/Pleistocene flood basalt related scoria and spatter cones,

rootless lava flows, and pit craters, A1 Haruj A1 Abyad, Libya," *Geolines*, pp. 98–103, 2003.

[7] E. S. Farahat, M. S. A. Ghani, A. S. Aboazom, and A. M. H. Asran, "Mineral chemistry of Al Haruj low-volcanicity rift basalts, Libya: implications for petrogenetic and geotectonic evolution," *Journal of African Earth Sciences*, vol. 45, no. 2, pp. 198–212, 2006.

[8] F. M. Ade-Hall, P. H. Reynolds, P. Dagley, A. G. Musset, T. B. Hubbard, and E. Klitsch, "Geophysical studies of North African Cenozoic volcanic areas 1—Haruj Assuad, Libya," *Canadian Journal of Earth Sciences*, vol. 11, pp. 998–1006, 1974.

[9] P. M. Vincent, "The evolution of Tibesti volcanic province, Eastern Sahara," in *African Magmatism and Tectonics*, T. N. Clifford and I. G. Gass, Eds., pp. 301–319, Oliver and Boyd, Edinburgh, UK, 1970.

[10] G. H. Goudarzi, "Structure-Libya," in *The Geology of Libya*, M. J. Salem and M. T. Busrewil, Eds., vol. 3, pp. 879–892, Academic Press, London, UK, 1980.

[11] F. Woller and F. Fediuk, "Volcanic rocks of Jabal as Sawada," *The Geology of Libya*, vol. 3, pp. 1081–1093, 1980.

[12] M. J. Le Bas, R. W. L. Maitre, A. Streckeisen, and B. Zanettin, "A chemical classification of volcanic rocks based on the total alkali-silica diagram," *Journal of Petrology*, vol. 27, no. 3, pp. 745–750, 1986.

[13] J. A. Winchester and P. A. Floyd, "Geochemical discrimination of different magma series and their differentiation products using immobile elements," *Chemical Geology*, vol. 20, pp. 325–343, 1977.

[14] M. T. Busrewil and W. J. Wadsworth, "Preliminary chemical data on the volcanic rocks of Al Haruj area, central Libya," in *The Geology of Libya*, M. J. Salem and M. T. Busrewil, Eds., pp. 1077–1080, Academic Press, London, UK, 1980.

[15] F. Woller, "Explanatory booklet. Geological map of Libya 1:250, 000, sheet," Al Fuqaha NG 33-3, Industrial Re-search Centre, Tripoli, Libya, 1984.

[16] S. Z. Harangi, *Petrology and Geochemistry of Basaltic Rocks, Al Haruj Area, Libya*, Industrial Research Centre, Tripoli, Libya, 2002.

[17] J.-M. Bardintzeff, C. Deniel, H. Guillou, B. Platevoet, P. Télouk, and K. M. Oun, "Miocene to recent alkaline volcanism between Al Haruj and Waw an Namous (southern Libya)," *International Journal of Earth Sciences*, vol. 101, no. 4, pp. 1047–1063, 2012.

[18] M. T. Busrewil, *The petrology and geochemistry of Tertiary volcanic rocks from Ghirian area, Tripolitania, Libya [Ph.D. thesis]*, University of Manchester, 1974.

[19] M. T. Busrewil and W. J. Wadsworth, "The basalts and associated lherzolite xenoliths of Waw-an-Namus volcano," *Libyan Journal of Science*, vol. 12, pp. 19–28, 1983.

[20] F. Woller, "Explanatory booklet. Geological map of Libya 1:250 000, sheet," Al Washkah NH 33-15, Industrial Research Centre, Tripoli, Libya, 1978.

[21] J. Vesely, "Explanatory booklet. Geological map of Libya 1:250, 000, Sheet," Zallah NH-33-16, Industrial Research Centre, Tripoli, Libya, 1985.

[22] K. Burke, "The African plate," *South African Journal of Geology*, vol. 99, pp. 339–340, 1996.

[23] K. Burke, "Origin of the cameroon line of volcano-capped swells," *Journal of Geology*, vol. 109, no. 3, pp. 349–362, 2001.

[24] G. Franz, C. Breitkreuz, D. A. Coyle et al., "The alkaline Meidob volcanic field (Late Cenozoic, northwest Sudan)," *Journal of African Earth Sciences*, vol. 25, no. 2, pp. 263–291, 1997.

[25] G. Y. Less, S. M. Turki, Z. Peregi et al., "Explanation booklet, Geological map of Libya, 1:250, 000. Sheet," Waw Al Kabir NG 33-12, Industrial Research Centre, Tripoli, Libya, 2006.

[26] D. Mckenzie and R. K. O'nions, "Partial melt distributions from inversion of rare earth element concentrations," *Journal of Petrology*, vol. 32, no. 5, pp. 1021–1091, 1991.

[27] M. Meschede, "A method of discriminating between different types of mid-ocean ridge basalts and continental tholeiites with the Nb1bZr1bY diagram," *Chemical Geology*, vol. 56, no. 3-4, pp. 207–218, 1986.

[28] B. Cabanis and M. Lecolle, "Le diagramme La/10- Y/15- Nb/8: un outil pour la discrimination des series volcaniques et la mise en evidence des processus de mélange et/ou de contamination crustale," *Comptes Rendus de l'Académie des Sciences. II*, vol. 309, pp. 2023–2029, 1989.

[29] D. A. Wood, J.-L. Joron, and M. Treuil, "A re-appraisal of the use of trace elements to classify and discriminate between magma series erupted in different tectonic settings," *Earth and Planetary Science Letters*, vol. 45, no. 2, pp. 326–336, 1979.

[30] J. F. Minster and C. J. Allègre, "Systematic use of trace elements in igneous processes—part III: inverse problem of batch partial melting in volcanic suites," *Contributions to Mineralogy and Petrology*, vol. 68, no. 1, pp. 37–52, 1978.

[31] M. Treuil, J. L. Joron, H. M. Jaffrezic, B. Villemant, and G. Calas, "Geochemie des elements hygromagmaphiles, coefficients de partage mineraux/liquide et proprietes structurales de ces elements dans les liquidsmagmatiques," *Bulletin Mineralogique*, vol. 102, pp. 402–409, 1979.

[32] J.-M. Cebriá and J. López-Ruiz, "A refined method for trace element modelling of nonmodal batch partial melting processes: the Cenozoic continental volcanism of Calatrava, central Spain," *Geochimica et Cosmochimica Acta*, vol. 60, no. 8, pp. 1355–1366, 1996.

[33] H. Nicholson and D. Latin, "Olivine tholeiites from krafla, Iceland: evidence for variations in melt fraction within a plume," *Journal of Petrology*, vol. 33, no. 5, pp. 1105–1124, 1992.

[34] P. Sprung, S. Schuth, C. Münker, and L. Hoke, "Intraplate volcanism in New Zealand: the role of fossil plume material and variable lithospheric properties," *Contributions to Mineralogy and Petrology*, vol. 153, no. 6, pp. 669–687, 2007.

[35] S.-S. Sun and W. F. McDonough, "Chemical and isotopic systematics of oceanic basalts: implications for mantle composition and processes," *Magmatism in the Ocean Basins*, pp. 313–345, 1989.

[36] A. W. Hoffman, "Sampling mantle heterogeneity through oceanic basalts: isotopes and trace elements," in *The Mantle and Core, 2, Treatise on Geochemistry*, R. W. Carlson, H. Holland, and K. K. Turekian, Eds., pp. 61–101, El Sevier-Pergamon, Oxford, UK, 2003.

[37] D. J. Chaffey, R. A. Cliff, and B. M. Wilson, "Characterization of the St Helena magma source," *Magmatism in the Ocean Basins*, vol. 42, pp. 257–276, 1989.

[38] A. P. Le Roex, "Geochemistry, mineralogy and magmatic evolution of the basaltic and trachytic lavas from Gough Island, South Atlantic," *Journal of Petrology*, vol. 26, no. 1, pp. 149–186, 1985.

[39] A. Zindler and S. Hart, "Chemical geodynamics," *Annual review of Earth and planetary sciences*, vol. 14, pp. 493–571, 1986.

[40] S. Pilet, J. Hernandez, P. Sylvester, and M. Poujol, "The metasomatic alternative for ocean island basalt chemical heterogeneity," *Earth and Planetary Science Letters*, vol. 236, no. 1-2, pp. 148–166, 2005.

[41] Y. Weinstein, O. Navon, R. Altherr, and M. Stein, "The role of lithospheric mantle heterogeneity in the generation of Plio-Pleistocene alkali basaltic suites from NW Harrat Ash Shaam (Israel)," *Journal of Petrology*, vol. 47, no. 5, pp. 1017–1050, 2006.